Journal Name

ARTICLE

Nanoparticles-cell association predicted by protein corona fingerprints

Received 00th January 20xx,
Accepted 00th January 20xx

DOI: 10.1039/x0xx00000x

www.rsc.org/

S. Palchetti,[a,b] L. Digiacomo,[a,c] D. Pozzi,[a,b] G. Peruzzi,[d] E. Micarelli,[e] M. Mahmoudi[f,g*] and G. Caracciolo[a,b*]

In a physiological environment (e.g., blood and interstitial fluids) nanoparticles (NPs) will bind proteins shaping a "protein corona" layer. The long-lived protein layer tightly bound to the NP surface is referred to as the hard corona (HC) and encodes information that controls NP bioactivity (e.g. cellular association, cellular signaling pathways, biodistribution, and toxicity). Decrypting this complex code has become a priority to predict the NP biological outcomes. Here, we use a library of 16 lipid NPs of various size (Ø ≈ 100-250 nm) and surface chemistry (unmodified and PEGylated) to investigate the relationships between NP physicochemical properties (nanoparticle size, aggregation state and surface charge), protein corona fingerprints (PCFs), and NP-cell association. We found out that none of the NPs' physicochemical properties alone was exclusively able to account for association with human cervical cancer cell line (HeLa). For the entire library of NPs, a total of 436 distinct serum proteins were detected. We developed a predictive-validation modeling that provides a means of assessing the relative significance of the identified corona proteins. Interestingly, a minor fraction of the HC, which consists of only 8 PCFs were identified as main promoters of NP association with HeLa cells. Remarkably, identified PCFs have several receptors with high level of expression on the plasma membrane of HeLa cells.

Introduction

When suspended in physiological milieu (e.g., blood and interstitial fluids) nanoparticles (NPs) will bind proteins that shape a "protein corona" layer on the NP external surface.[1-5] This corona, as described by the types of serum proteins and their abundance on the NP surface, depends on both the NP physicochemical properties[6, 7] and the blood protein source.[3, 8, 9] Recent developments have revealed that corona decoration is largely affected by the type of human patient from which the plasma is obtained.[9, 10] Temperature[11, 12] and exposure time[13, 14] have been also identified as strategic factors shaping both the NP physicochemical properties and the NP-corona. The corona is composed by an outer short-lived layer in dynamical equilibrium with the surrounding environment (the "soft corona") and a long-lived layer tightly bound to the NP surface, referred to as the hard corona (HC).[15] Being the NP interface seen by cells, the HC is thought to give a new identity to the NP by encoding information that controls NP bioactivity (e.g. cellular association).[1, 15-17] Thus, interpreting such cryptic code has become a priority to predict the NP biological outcomes. To this end, a number of quantitative structure–activity relationships (QSARs) have been successfully developed.[18] Physicochemical properties used as descriptors are those that characterize the biological identity of NPs suspended in a biological fluid, i.e. their size, zeta-potential, and aggregation state.[2, 18] In addition, the relative abundance of the identified proteins adsorbed on the NP surface is used as a "fingerprint" to characterize the HCs.

For some classes of inorganic nanomaterials (e.g. gold NPs) correlations of HC fingerprints with cell association were demonstrated.[2, 18, 19] Currently, organic nanomaterials such as liposomes and polymers are tested for a wide range of applications, ranging from nanobiomedicine to consumer products. In any cases, clear-cut explanation of the role played by their HC in mediating cell association is still missing.

In this work, we employed a compositionally diverse library of 16 negatively or positively charged lipid NPs of various size (Ø

[a] Department of Molecular Medicine, "Sapienza" University of Rome, Viale Regina Elena 291, 00161 Rome, Italy.
[b] Istituti Fisioterapici Ospitalieri, Istituto Regina Elena, Via Elio Chianesi 53, 00144 Rome, Italy.
[c] School of Biosciences and Veterinary Medicine, University of Camerino, Via Gentile III da Varano, 62032 Camerino (MC), Italy.
[d] Istituto Italiano di Tecnologia, CLNS@Sapienza, Viale Regina Elena 291, 00161, Rome, Italy
[e] Department of Biology, University of Rome Tor Vergata, Via della Ricerca Scientifica 1, 00133 Rome, Italy.
[f] Nanotechnology Research Center, Faculty of Pharmacy, Tehran University of Medical Sciences, Tehran, Iran.
[g] Stanford Cardiovascular Institute and Division of Cardiovascular Medicine, Stanford University, School of Medicine, California, USA.
*E-mail: giulio.caracciolo@uniroma1.it; Mahmoudi@stanford.edu.

Electronic Supplementary Information (ESI) available: **Table S1.** Cell viability (%) and cell association of the different nanoparticles used. **Table S2.** Total number of identified proteins on the different nanoparticles used. **Table S3-S19.** Top 25 most abundant corona proteins identified in the protein corona of nanoparticles NP1-NP16 following 1 hour incubation with HP. **Table S20.** List of descriptors used. **Table S21.** Potential targets of protein corona fingerprints with its own interaction score (mentha) and the expression median value in Hela cells. **Figure S1-S2.** Effect of exposure to human plasma on size and zeta potential of NPs. **Figure S3.** Predictive modeling of nanoparticle-cell association.
See DOI: 10.1039/x0xx00000x

Table 1. Nanoparticle characterization. The average size of 16 nanoparticles with different surface chemistry was determined in buffer by DLS. Plasma measurements were performed 1 hour post-exposure to human plasma (HP), followed by plasma separation and subsequent washing as described in Materials and Methods section. Zeta-potential of the different nanoparticles in buffer and after 1 hour post-exposure to HP. Values are mean ± s.d. from three independent experiments. Micrograms of proteins bound to liposomes after 1 hour incubation with HP.

	Surface chemistry	DLS hydrodynamic diameter ± s.d. (nm) (PDI)		Zeta potential ± s.d. (mV)		Protein Assay (ug/ul)
		In Buffer	Plasma	In Buffer	Plasma	Plasma
NP1	Cationic, plain	112 ± 11 (0.17)	228 ± 4 (0.23)	48.5 ± 0.9	-17.9 ± 0.7	9.7 ± 1.1
NP2	Cationic, plain	135 ± 8 (0.14)	259 ± 21 (0.12)	30.1 ± 3.4	-19.3 ± 1.8	5.06 ± 0.45
NP3	Cationic, plain	128 ± 17 (0.11)	150 ± 6 (0.15)	47.4 ± 0.9	-23.0 ± 1.1	10.55 ± 0.89
NP4	Cationic, plain	131 ± 7 (0.10)	182 ± 13 (0.16)	26.1 ± 2.9	-25.5 ± 1.4	5.51 ± 0.54
NP5	Cationic, plain	157 ± 10 (0.17)	211 ± 14 (0.23)	58.2 ± 4.3	-28.5 ± 2.3	6.70 ± 0.62
NP6	Cationic, plain	108 ± 4 (0.14)	216 ± 2 (0.22)	34.5 ± 5.5	-17.9 ± 2.3	4.02 ± 0.43
NP7	Cationic, plain	125 ± 10 (0.18)	207 ± 12 (0.21)	46.2 ± 2.2	-20.4 ± 4.5	5.47 ± 0.56
NP8	Cationic, plain	254.6 ± 22.9 (0.12)	329 ± 12 (0.15)	33.1 ± 2.4	-15.4 ± 1.2	4.36 ± 0.28
NP9	Cationic, plain	193.4 ± 15.2 (0.13)	236 ± 18 (0.19)	42.1 ± 1.2	-19.3 ± 1.4	3.93 ± 0.27
NP10	Zwitterionic, plain	191 ± 23 (0.11)	301 ± 18 (0.15)	-8.4 ± 1.9	-22.1 ± 2.3	2.94 ± 0.32
NP11	Anionic, plain	136 ± 1 (0.10)	152 ± 12 (0.15)	-26.6 ± 0.2	-18.2 ± 0.8	8.50 ± 1.09
NP12	Anionic, plain	126 ± 23 (0.11)	171 ± 11 (0.13)	-14.2 ±1.1	-28.6 ± 1.4	4.06 ± 0.51
NP13	Cationic, plain	144 ± 4 (0.09)	178 ± 6 (0.14)	30.2 ± 2.9	-29.3 ± 3.5	4.91 ± 0.64
NP14	Cationic, PEGylated	114 ± 1 (0.08)	137 ± 6 (0.16)	18.1 ± 3.3	-13.9 ± 0.6	2.70 ± 0.21
NP15	Cationic, PEGylated	123 ± 6 (0.12)	169 ± 6 (0.17)	17.9 ± 1.2	-24.5 ± 1.2	1.50 ± 0.03
NP16	Cationic, PEGylated	103.2 ± 9.7 (0.09)	115 ± 1 (0.13)	9.9 ± 2.2	-13.2 ± 0.9	1.10 ± 0.12

≈ 100-250 nm) and surface chemistry (unmodified, PEGylated) and we let them interact with human plasma (HP). Thus, the selected model systems are relevant for nanobiomedicine and nanotoxicology. NP coronas were highly complex in composition, each of them being composed of about 200 different proteins. Here we show that a minor fraction of the HC, which consists of only 8 proteins, controls cell association of selected NPs with human cervical cancer cell line (HeLa) cells. These cells are widely used as a model to study fundamental NP-cell interactions.

Results and Discussion

Particles were incubated with undiluted HP for 1 hour at 37 °C, separated from plasma components by centrifugation, washed and resuspended in protein-free medium. It should be noted that plasma is a better model than serum for the in vivo human environment, since not only key blood coagulation factors are absent in serum but also the plasma is the real protein source that NPs may "see" in vivo.[20] HC-coated NPs were thoroughly characterized by dynamic light scattering (DLS) and zeta-potential measurements (Table 1). Due to the formation of protein corona layer, the HC-coated NPs were bigger in size than bare NPs. Increase in size ranged between 10 and 120 nm and, for 13 of 16 formulations, was not compatible with particle aggregation[21, 22] (Figure S1 in the Electronic Supplementary Information, ESI). For monodisperse HC-coated NPs the change in size after plasma exposure changes monotonously with hydrodynamic diameter of NPs after incubation with human plasma (Figure S1 in the ESI).

HC-coated NPs, irrespective of the bare particles' negative or positive surface functionalization, display an overall negative charge (Table 1). After plasma exposure the variation in zeta-potential is a linear function of the zeta-potential after synthesis (Figure S1 in the ESI). Plasma incubation resulted in a "normalization" of the zeta-potential to an average value of about -21 ± 5 mV independently of the pristine surface charge. Most plasma proteins carry a net negative charge at physiological pH 7.4. Upon adsorption, the anionic plasma proteins impart a net negative charge to the NP. It was suggested that negatively charged particles attract primarily positively charged proteins and vice versa. However, the observed behavior, which was previously detected for metal NPs with varying physicochemical properties,[2] indicates that the main driving force in the protein-NP interaction is not merely electrostatic.

There is a current debate as to whether NP's physicochemical features such as size and surface charge affect the NP-cell association. Previous studies proposed a size-dependent mechanism of NP-cell association.[23] Other studies reported that the surface properties of different NPs were as relevant as particle size for cellular uptake.[24] HC-coated NPs were highly heterogeneous both in size and zeta-potential (Table 1). Thus, the chosen library of NPs was particularly attractive to investigate the role of these factors on the NP-cell association. When HeLa cells were exposed to HC-coated NPs, no sign of cytotoxicity was detected using MTT approach (Table S1 in the ESI). Cell association of fluorescently labeled HC-coated NPs, which includes internalization of the NPs and adhesion to the cell membrane,[18] was evaluated by flow cytometry. Notably, significant differences in cell adhesion were observed between formulations with percentage of fluorescent cells varying between ≈ 1 and 100% (Table S1 in the ESI), which underlines the necessity to dissect molecular mechanisms responsible for NP-cell association. NP-cell association was insensitive to size, zeta-potential, and aggregation state (Figure S2 in the ESI). Collectively, our analyses demonstrate that none of the NPs' physicochemicalproperties alone was able exclusively to account for association with HeLa cells. On the other side, increasing

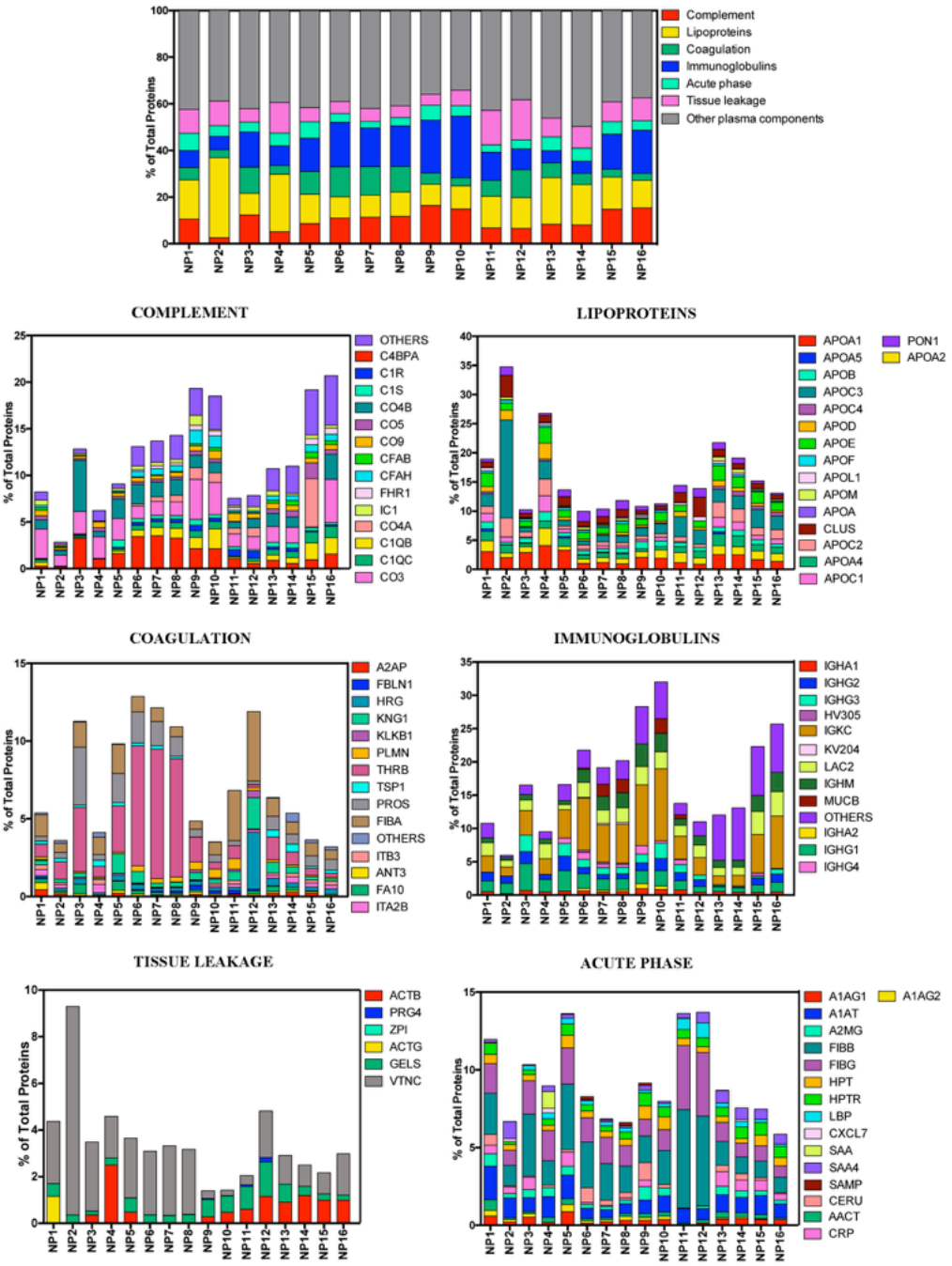

Figure 1. Proteins identified in the nanoparticles' coronas by quantitative LC-MS. The relative protein abundance of proteins is shown. The concentration of proteins involved in complement activation, coagulation, acute phase and tissue leakage were particularly strongly affected by nanoparticle physicochemical properties. Complement activation proteins bound preferentially to NP9, NP10, NP15 and NP 16. Lipoproteins bound preferentially to NP2 and NP4, whereas enhanced binding of tissue leakage proteins was observed for NP2. Although immunoglobulins are present in high amounts in the plasma, these proteins displayed distinct binding to all nanoparticles with RPA ranging from 5% (NP) to 30% (NP). Detailed values for all individual proteins are available in Tables S3 and S4 in the ESI.

evidence has shown that the protein corona regulates NP-cell recognition, and hence plays important roles in modulating NP's bioactivity.[9, 13] For example, the adsorption of proteins on NPs has been shown to impact on the specificity of NPs to targeted cells, resulting in the loss or reduction of the targeting capability of surface functionalized NPs.[25, 26] On the flip side, a long-standing corona with receptor-binding sites could stimulate association with the cell hence triggering particle endocytosis and intracellular cargo delivery. Thus, prediction of the biological impact of the adsorbed protein corona requires a full characterization of its composition.

The HC of the entire collection of NP was quantitatively characterized by nano liquid chromatography tandem mass spectrometry (nanoLC-MS/MS).[27-30] The accuracy and reproducibility of the nanoLC MS/MS characterization was established using 3 independent experimental replicates and 3 technical replicates for each of the experimental

ones. Over the entire library, N=436 distinct proteins were identified and quantified. For each NP formulation, the total number of identified proteins and their relative abundance did depend on both formulation and surface ligand chemistry (Table S2 in the ESI). On average, each formulation adsorbed 195 ± 33 distinct plasma proteins. Tables S3-S19 in the ESI lists the most-abundant proteins for each NP. Our data verifies that the relative abundance of proteins in the corona of lipid NP does not, generally, reproduce their relative abundance in plasma because low abundance proteins are enriched on the NP surface. Previous investigations have shown that the protein corona of inorganic NPs appears to follow a general structure, with the top 3 most abundant proteins representing on average roughly 55%.[2] In this regard, the protein corona of lipid NPs seems to be more heterogeneous in composition with 25 hits representing on average about 60%.

To facilitate their rational identification, proteins were categorized bioinformatically according to biological processes of the blood system (Figure 1). The relative protein abundance (RPA) of biologically relevant proteins such as, proteins involved in complement activation, coagulation, immune response, acute phase and tissue leakage were particularly affected by NP's characteristics. In particular, while immunoglobulins are present in high concentrations in the plasma, these proteins exhibited only moderate adsorption to most NP formulations. A functionally diverse group of plasma proteins highly enriched in the coronas of lipid NPs are the apolipoproteins. Apolipoproteins were enriched significantly in the coronas of NP1-4 and are likely to trigger NP-induced biological responses. Particularly, *APOA-I*, *APOB,* and *APOE* enable targeted delivery of drugs to the lung tumors,[31] enhance the uptake of lipid NP by hepatocytes[32] and help NPs towards crossing the blood brain barrier.[33, 34]

Given the involvement of corona proteins in many biological processes, their identification and quantification is a fundamental step towards prediction of NP behavior in vivo. In this regard, protein abundance is not the only factor to consider. Indeed, highly enriched proteins might be unfolded[35] or their functional motifs buried inside.[28] On the other side, poorly enriched but exposed proteins could favorably interact with receptors of target cells. These arguments highlight how prediction of NP-cell adhesion will require more than just the knowledge of the protein corona composition, but accurate mapping protein-binding sites on the NP corona.[36] Many receptors exist on cell membranes such as folate and transferrin receptors, growth factor receptors and integrins. Thus, if multiple epitopes of different corona proteins are exposed, they could be recognized by different cell receptors. As a matter of fact, simultaneous binding of multiple ligands to multiple cell receptors naturally occurs in many biological systems. The multivalent effect, i.e. the multivalent binding between multiple ligands and multiple receptors is critical to many cellular processes and can confer several advantages such as higher biological recognition, improved and tight binding.[37] An example of polyvalent interactions relevant to human biology is given by the influenza virus that binds to cells by multiple interactions.[38] Of note, a growing number of viruses have been found to use many types of receptors for the attachment to target cells and the same mechanism is still valid for bacteria-cell interactions.[38]

Deciphering which corona proteins play a role on NP cellular association is a challenging question since mastering the NP-protein corona itself could be a novel means to target diseases instead of chemical grafting. Cells could therefore interact with protein-NP complexes via a multitude of different receptors, which have saturable binding sites. In this regard, association of HC-coated NPs with target cells would resemble that of ligands/antibodies-linked NPs targeting several membrane receptors simultaneously. When ligand-grafted NPs are administered to cells, cellular association shows a typical saturable dependence on the NP concentration. According to all these evidences was the idea to identify specific protein corona fingerprints that let NP-cell association exhibit saturable dependence on their abundance. To determine which protein fingerprints promote cell association, a two-step procedures was used. In the first step, list of predictors was created (Table S20 in the ESI). The list comprised n=14 corona proteins that are usually categorized as being positively correlated with NP cell association[18 22, 39, 40] and represented on average about 60% of the PC (Table S20 in the ESI). Then, we developed a m×n Pij matrix, that identifies the relative amount of the protein j within the corona of the i-th formulation. The cellular association Ai of the i-th formulation can be regarded as a function of some specific contributions among the n measured protein abundances, i.e.

$$A_i = f\left(\sum_{j\in\Gamma} P_{ij}\right) \qquad (1)$$

Where Γ indicates the set of indexes corresponding to the proteins that are included in the list of predictors. In the first step (hereafter named 'step I'), the aim was to determine the k elements in Γ (k≤n), which best approximate A to a saturation function f. Since the association is defined as percentage of fluorescent cells, f must have values within the range [0,100]

$$f(x) = 100[1 - exp\{-b(x - x_0)\}] \qquad (2)$$

The best ensemble Γ was evaluated by means of least square method, i.e. by fitting A through f, where the independent variable is represented by the partial sums of the protein abundances. Thus, for each k-value, $\binom{n}{k}$ fitting curves were obtained, each of them for any possible sum of k terms belonging to the list of n descriptors.

Among the $\sum_{k=1}^{n}\binom{n}{k}$ combinations, prediction accuracy was evaluated in terms of fitting determination coefficient R^2.

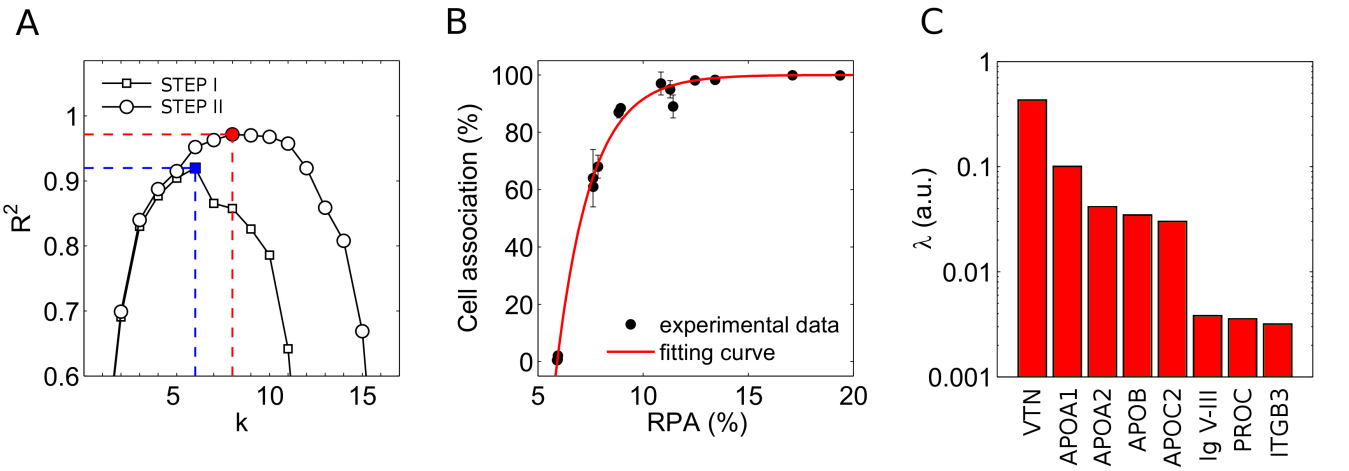

Figure 2. (A) Prediction accuracy (R^2) as a function of increasing number of descriptors (k). In Step I, n=14 descriptors are chosen among the N=436 proteins identified in the nanoparticle-coronas. For each k-value, all their $\binom{n}{k}$ possible combinations are explored. In step I, the highest accuracy was achieved with k_I=6 (blue square, R^2=0.920). In Step II a one-at-a-time sensitivity analysis was performed with the aim of exploring the involvement of the (N-n) corona proteins that were excluded in Step I. Step II resulted in the inclusion of two more PCFs. Red circle identifies the "turning-point" where the prediction accuracy was maximum (R^2=0.972). This was achieved with a final set of k_{II}=8 proteins. (B). Cellular association of NPs as a function of the total protein abundance of the 8 PCFs identified in the two-step procedure described in panel A. (C) Ranking coefficient of the 8 PCFs.

As shown in the panel A of Figure 2, the prediction accuracy R^2 was highly dependent on k and exhibits a "turning-point" at k_I=6. Hence, step I of the procedure allowed us to determine a set of 6 elements (*Vitronectin*, *APOA1*, *APOA2*, *APOB*, *APOC2*, *Integrin beta3*), which promote NP association to HeLa cells. The extremely high computational cost of step I did not allow us to include all the detected proteins (i.e. N=436) within the starting set of descriptors. Step II was devoted to overcoming this limit. To this end, we adopted a one-at-a-time sensitivity analysis aimed at exploring the involvement of all the (N-n) proteins that were excluded in Step I (a detailed description of the procedure is given in Figure S3 panel A in the ESI). Step II resulted in the boost of prediction accuracy (Figure 2, panel A) by inclusion of two more PCFs. The final set of k_{II}=8 proteins ensured a high prediction accuracy (Figure 2, panel B). It was noteworthy that, of the entire pool of possible descriptors (N=436 proteins), a very small set of 8 PCFs (*Vitronectin*, *APOA1*, *APOA2*, *APOB*, *APOC2*, *Ig heavy chain V-III region BRO*, *Vitamin K-dependent protein*, *Integrin beta3*) demonstrated the greatest impact on the correlation of NP cell association. Notably, the same proteins were also identified in previous works as being highly relevant to correlating NP-cell association.

Further implication of the procedure was the production of a ranking coefficient, I, by which all the corona proteins were classified in their ability to promote cell association (Figure 2 panel C and Figure S3 panel B in the ESI). Vitronectin was the most relevant PCF followed by *APOA1*, *APOA2*, *APOB* and *APOC2*. The most relevant protein seemed to be Vitronectin is a glycoprotein and, together with fibronectin, is one of the major cell adhesion proteins in plasma. Vitronectin interact with glycosaminoglycans and proteoglycans and is recognized by certain members of the integrin family such as a_vb_3. Vitronectin contains the Arg-Gly-Asp (RGD) motif in the Somatomedin B domain (20–63 region) that is specifically recognized by $\alpha v\beta_3$ integrins, which are overexpressed on many solid tumors and in tumor neovasculature. *APOA1*, *APOA2* interact selectively and non-covalently with the apolipoprotein receptor.[41] *APOB* has been reported to act as a ligand for LDL receptors in various cells. *APOC2* is secreted in plasma where it is a component of very low-density lipoproteins (VLDL) and chylomicrons. *APOC2* is an activator of lipoprotein lipase (LPL) and its structure is predicted to contain 3 helical regions, which are thought to be involved in phospholipid binding. Interestingly, this finding seems to suggest that not only cell receptors, but also lipids of the plasma membrane, could be involved in the corona-mediated endocytosis of NPs.

This aspect deserves further consideration and is being currently investigated in our laboratory. On the other side, the ranking coefficients of *Ig heavy chain V-III region BRO*, *Vitamin K-dependent protein* and *Integrin beta3* were lower suggesting a minor role of those proteins on NP-cell association. To rationalize the identification of the PCFs potentially associated with the protein corona components, a bioinformatics analysis of protein cell receptors was performed (detailed information can be found in the Materials and Methods section). In brief, for each protein belonging to the selected set of PCFs, we determined its interaction partners (and levels of expression) on the external side of the plasma membrane of Hela cells. Remarkably, we found out that our two-step procedure resulted in the identification of PCFs with several receptors on the plasma membrane of HeLa cells (Table S21 in the ESI). For each PCF, at least one cell receptor exhibited a high level of expression as quantified by the GENEVESTIGATOR tool.

Materials and Methods

Nanoparticle preparation

Cationic lipids 1,2-dioleoyl-3-trimethylammonium-propane (DOTAP) and (3β-[N-(N',N'-dimethylaminoethane)-carbamoyl])-cholesterol (DC-Chol), zwitterionic lipids dioleoylphosphocholine (DOPC), dioleoylphosphatidylethanolamine (DOPE), DOPE-polyethyleneglycol (PEG)-1K, DOPE-PEG-2K, DOPE-PEG-5K, 1,2-distearoyl-sn-glycero-3-phosphocholine (DSPC), 1,2-dipalmitoyl-sn-glycero-3-phosphocholine (DPPC) and 1,2-diarachidoyl-sn-glycero-3-phosphocholine (20:0 PC) and anionic lipids 1,2-dioleoyl-sn-glycero-3-phospho-(1'-rac-glycerol) (DOPG) and 1,2-dioleoyl-sn-glycero-3-phosphate (DOPA) were purchased from Avanti Polar Lipids (Alabaster, AL). Sphingosine, Cholesterol (Chol) and DOPE labeled with 7-nitrobenzofurazan (NBD) were purchased from Sigma-Aldrich (St. Louis, MO, USA). All lipids were used without further refinement. Sixteen nanoparticle formulations (indicated as NP1-NP16) were prepared at desired molar ratios. Each lipid was dissolved in chloroform and the solvent was evaporated under a vacuum for at least 24 hours. Lipid films were hydrated to obtain a final lipid concentration of 1 mg/mL with ultrapure water for size, zeta-potential, cytotoxicity and flow cytometry experiments. For proteomics experiments lipid films were hydrated with a dissolving buffer (Tris–HCl, pH 7.4, 10 mmol L^{-1}; NaCl, 150 mmol L^{-1}; EDTA, 1 mmol L^{-1}) and stored at 4 °C. The obtained liposome solutions were extruded 20 times through a 0.1μm polycarbonate carbonate filter with the Avanti Mini-Extruder (Avanti Polar Lipids, Alabaster, AL).

Size and zeta-potential

Dynamic light scattering experiments and laser Doppler electrophoresis were carried out to measure nanoparticles' size and zeta-potential. All the measurements were made at 25°C on a Zetasizer Nano ZS90 spectrometer (Malvern, U.K.) equipped with a 5 mW HeNe laser (wavelength λ = 632.8 nm) and a non invasive back-scattering optical setup (NIBS). For each sample, the detected intensity was processed by a digital logarithmic correlator, which computes a normalized intensity autocorrelation functions. Then, the distribution of the diffusion coefficient D was obtained by using the CONTIN method.[42] Finally, D was converted into an effective hydrodynamic radius RH through the Stokes-Einstein equation: $R_H = K_BT/(6\pi\eta D)$, where K_BT is the system's thermal energy and η represents the solvent viscosity. The electrophoretic mobility measurements were performed by means of the same apparatus used for size experiments. The mobility u of nanoparticles experiencing an external electric field was detected and converted into the zeta-potential by using the Smoluchowski relation: zeta-potential = uη/ε, where η and ε are respectively the viscosity and the permittivity of the solvent phase. Sample solutions of bare liposomes were diluted 1:100 with distillated water. Particles (10 mL) were incubated with undiluted HP (10 mL) for 1 hour at 37 °C, separated from plasma components by centrifugation, washed and resuspended in protein-free medium (20 mL). Size and zeta-potential experiments of NP-HP complexes were carried out by diluting 20 mL of NP-HP complexes, with 980 mL of distillated water. Results are given as mean ± standard deviation of five replicates.

Cell culture

Human cervical cancer cell line (HeLa) was purchased from ATCC (Manassas, VA, USA). HeLa cells were maintained in Eagle's Minimum Essential Medium (EMEM) supplemented with 2 mM L-glutamine, 100 IU/mL penicillin/streptomycin, 1 mM sodium pyruvate, 10 mM hepes, 1.5 mg/L sodium bicarbonate and 10% fetal bovine serum (FBS).

Protein assay

We used Protein Assay reagent (Pierce, Thermo Scientific, Waltham, MA, USA) to measure the amount of bound proteins on liposomes after incubation with HP, according to manufacturer's protocol. Briefly, after incubation of each NP formulation with HP for 1 hour at 37°C, NP-HP complexes were centrifuged at 14000 rpm for 15 minutes at 4°C and washed 3 times with PBS. The resulting pellet was resuspended in urea 8 mol/L NH_4CO_3 50 mmol/. Ten μL of each sample was placed into a 96-multiwell plate adding then 150 μL of Protein Assay reagent. The multiwall was incubated at room temperature for 5 minutes and then mixed on a plate shaker. The absorbance of each sample, blank and standards was measured with the Glomax Discover System (Promega, Madison, WI, USA) at 660 nm. The protein concentration was calculated using the standard curve and all the measures were made in triplicate.

Cell viability

To examine the possible cytotoxicity resulting from bare NPs, cell viability of HeLa cells was evaluated by using 3-(4,5-dymethyl thiazol 2-y1)-2,5-diphenyl tetrazolium bromide (MTT, mitochondrial respiration analysis; Sigma-Aldrich), according to Mosmann protocol. Briefly, HeLa cells were seeded on 96-wells plate (10.000 cells/well). 24 hours after seeding, cells were treated with 10 μg/mL of each NP formulation in Optimem medium (Life Technologies, Carlsbad, CA) for 24 hours. Then, MTT was added to each well at the final concentration of 0.5 mg/mL. After 4 hours of incubation at 37°C, the formazan salt was dissolved with 100 μL isopropylic alcohol and the absorbance of each well was measured with Glomax Discover System (Promega, Madison, WI, USA) at 570 nm. Cell viability was calculated for each treatment as "OD of treated cells/OD of control cells" ×100. All the measures were made in triplicate. Results are given as mean ± standard deviation.

Flow cytometry

To determine cellular uptake of bare NPs in HeLa cells, each formulation was synthesized with the addition of DOPE-NBD, with the concentration of fluorescently labeled NBD-DOPE of 7x10-3 mg/mL (fluorescent lipid/total lipid molar

ratio = 5/1000) (excitation 488 nm, emission 530 nm). HeLa cells were seeded in 12-well plate (200.000 cells/mL) and, after 24 hours, cells were treated with 10 µg/mL of NBD-labeled NPs in Optimem medium for 3 hours. Then, cells were detached with trypsin/ethylenediaminetetraacetic acid (EDTA), washed two times with cold PBS, and acquired using a cytometer. Fluorescence-activated cell sorting (FACS) analysis was performed using BD LSRFortessa equipped with 488 nm laser and with DIVA software (BD Biosciences, San Jose, CA, USA). HeLa cells were first gated using forward vs side scatter (FSC vs SSC) strategy to exclude debris (low events) and then analyzed for the specific 530 nm emission (FITC channel). Data were analyzed using FlowJo software (FlowJo LLC data analysis software, Ashland, OR, USA). The percentage of FITC positive cells indicated NP-cell interaction (Cell association %, Table S1 in the ESI).

Cell receptors of protein corona fingerprints

A computational procedure, starting from a protein belonging to nanoparticle corona, allows identifying its interaction partners localized on plasma membrane. The procedure approach is based on two steps: i) identification of the corona protein interaction partners by accessing to the Mentha database of experimentally validated protein-protein interactions[43]; then, ii) the list of interacting proteins is sorted according to a score calculated by a function based on Gene Ontology annotations.[44, 45] Finally, the gene expression profile of proteins, deemed to be localized on plasma membrane, has been consulted by means of the GENEVESTIGATOR tool.[46]

Conclusion

A combinatorial library of 16 negatively or positively charged lipid NPs of various size and surface was employed to investigate the correlation between NP-cell association, NP physicochemical properties and protein corona fingerprints. Collectively, our analyses demonstrate that none of the NPs' physicochemical properties alone was able exclusively to account for association with HeLa cells. Among 436 identified plasma proteins, *Vitronectin*, *APOA1*, *APOA2*, *APOB*, *APOC2*, *Ig heavy chain V-III region BRO*, *Vitamin K-dependent protein*, *Integrin beta3* were identified as being significant protein corona fingerprints for correlating NP cell association. The developed predictive modeling provides a means of evaluating the substance of the identified corona proteins in promoting NP-cell association. Identification of protein corona fingerprints will be useful in developing NP with targeted NP protein adsorption and will open the intriguing possibility to manipulate the corona composition by nanoparticle design.

Acknowledgements

SP, DP and GC acknowledge support by the Italian Minister of Health (Progetto Giovani Ricercatori 2011-2012, Grant No. GR-2011-02350094). Prof. Aldo Laganà and his group are thankfully acknowledged for fruitful collaboration over the years. MM would like to thank Tehran University of Medical Sciences for supporting this work (Grant No. 94-04-33-31032).

Notes and references

1. M. P. Monopoli, C. Åberg, A. Salvati and K. A. Dawson, *Nature nanotechnology*, 2012, **7**, 779-786.
2. C. D. Walkey and W. C. W. Chan, *Chemical Society Reviews*, 2012, **41**, 2780-2799.
3. P. Del Pino, B. Pelaz, Q. Zhang, P. Maffre, G. U. Nienhaus and W. J. Parak, *Materials Horizons*, 2014, **1**, 301-313.
4. M. J. Hajipour, S. Laurent, A. Aghaie, F. Rezaee and M. Mahmoudi, *Biomaterials Science*, 2014, **2**, 1210-1221.
5. G. Caracciolo, *Nanomedicine: Nanotechnology, Biology and Medicine*, 2015, **11**, 543-557.
6. M. P. Monopoli, D. Walczyk, A. Campbell, G. Elia, I. Lynch, F. Baldelli Bombelli and K. A. Dawson, *Journal of the American Chemical Society*, 2011, **133**, 2525-2534.
7. A. L. Capriotti, G. Caracciolo, C. Cavaliere, P. Foglia, D. Pozzi, R. Samperi and A. Laganà, *Journal of Proteomics*, 2012, **75**, 1924-1932.
8. G. Caracciolo, D. Pozzi, A. L. Capriotti, C. Cavaliere, S. Piovesana, G. La Barbera, A. Amici and A. Laganà, *Journal of Materials Chemistry B*, 2014, **2**, 7419-7428.
9. M. J. Hajipour, J. Raheb, O. Akhavan, S. Arjmand, O. Mashinchian, M. Rahman, M. Abdolahad, V. Serpooshan, S. Laurent and M. Mahmoudi, *Nanoscale*, 2015, **7**, 8978-8994.
10. V. Colapicchioni, M. Tilio, L. Digiacomo, V. Gambini, S. Palchetti, C. Marchini, D. Pozzi, S. Occhipinti, A. Amici and G. Caracciolo, *The International Journal of Biochemistry & Cell Biology*, 2015.
11. D. Pozzi, H. Amenitsch, R. Caminiti and G. Caracciolo, *Chemical Physics Letters*, 2006, **422**, 439-445.
12. M. Mahmoudi, A. M. Abdelmonem, S. Behzadi, J. H. Clement, S. Dutz, M. R. Ejtehadi, R. Hartmann, K. Kantner, U. Linne and P. Maffre, *ACS nano*, 2013, **7**, 6555-6562.
13. A. L. Barrán-Berdón, D. Pozzi, G. Caracciolo, A. L. Capriotti, G. Caruso, C. Cavaliere, A. Riccioli, S. Palchetti and A. Laganaì, *Langmuir*, 2013, **29**, 6485-6494.
14. S. Tenzer, D. Docter, J. Kuharev, A. Musyanovych, V. Fetz, R. Hecht, F. Schlenk, D. Fischer, K. Kiouptsi and C. Reinhardt, *Nature nanotechnology*, 2013, **8**, 772-781.
15. M. Lundqvist, J. Stigler, G. Elia, I. Lynch, T. Cedervall and K. A. Dawson, *Proceedings of the National Academy of Sciences*, 2008, **105**, 14265-14270.
16. E. Mahon, A. Salvati, F. Baldelli Bombelli, I. Lynch and K. A. Dawson, *Journal of Controlled Release*, 2012, **161**, 164-174.
17. G. Caracciolo, F. Cardarelli, D. Pozzi, F. Salomone, G. Maccari, G. Bardi, A. L. Capriotti, C. Cavaliere, M. Papi and A. Laganà, *ACS applied materials & interfaces*, 2013, **5**, 13171-13179.

18. C. D. Walkey, J. B. Olsen, F. Song, R. Liu, H. Guo, D. W. H. Olsen, Y. Cohen, A. Emili and W. C. Chan, *ACS nano*, 2014, **8**, 2439-2455.
19. C.-Y. Shao, S.-Z. Chen, B.-H. Su, Y. J. Tseng, E. X. Esposito and A. J. Hopfinger, *Journal of chemical information and modeling*, 2013, **53**, 142-158.
20. V. Mirshafiee, R. Kim, M. Mahmoudi and M. L. Kraft, *The international journal of biochemistry & cell biology*, 2015.
21. R. M'Hallah, A. Alkandari and N. Mladenovic, *Computers & Operations Research*, 2013, **40**, 603-615.
22. D. Pozzi, G. Caracciolo, L. Digiacomo, V. Colapicchioni, S. Palchetti, A. L. Capriotti, C. Cavaliere, R. Z. Chiozzi, A. Puglisi and A. Laganà, *Nanoscale*, 2015, **7**, 13958-13966.
23. W. Jiang, B. Y. Kim, J. T. Rutka and W. C. Chan, *Nature nanotechnology*, 2008, **3**, 145-150.
24. E. Fröhlich, *International journal of nanomedicine*, 2012, **7**, 5577.
25. V. Mirshafiee, M. Mahmoudi, K. Lou, J. Cheng and M. L. Kraft, *Chemical Communications*, 2013, **49**, 2557-2559.
26. A. Salvati, A. S. Pitek, M. P. Monopoli, K. Prapainop, F. B. Bombelli, D. R. Hristov, P. M. Kelly, C. Åberg, E. Mahon and K. A. Dawson, *Nature nanotechnology*, 2013, **8**, 137-143.
27. G. Caracciolo, D. Pozzi, A. L. Capriotti, C. Cavaliere and A. Laganà, *Journal of Nanoparticle Research*, 2013, **15**.
28. G. Caracciolo, S. Palchetti, V. Colapicchioni, L. Digiacomo, D. Pozzi, A. L. Capriotti, G. La Barbera and A. Laganà, *Langmuir*, 2015, **31**, 10764-10773.
29. G. Caracciolo, D. Pozzi, A. L. Capriotti, C. Cavaliere, S. Piovesana, H. Amenitsch and A. Laganà, *RSC Advances*, 2015, **5**, 5967-5975.
30. D. Pozzi, G. Caracciolo, A. L. Capriotti, C. Cavaliere, G. La Barbera, T. J. Anchordoquy and A. Laganà, *Journal of proteomics*, 2015, **119**, 209-217.
31. S. K. Kim, M. B. Foote and L. Huang, *Biomaterials*, 2012, **33**, 3959-3966.
32. S. I. Kim, D. Shin, H. Lee, B.-Y. Ahn, Y. Yoon and M. Kim, *Journal of hepatology*, 2009, **50**, 479-488.
33. T. Wang, J. R. Upponi and V. P. Torchilin, *International Journal of Pharmaceutics*, 2012, **427**, 3-20.
34. M. Mahmoudi, S. Sheibani, A. S. Milani, F. Rezaee, M. Gauberti, R. Dinarvand and H. Vali, *Nanomedicine*, 2015, **10**, 215-226.
35. Z. J. Deng, M. Liang, I. Toth, M. J. Monteiro and R. F. Minchin, *ACS nano*, 2012, **6**, 8962-8969.
36. P. M. Kelly, C. Åberg, E. Polo, A. O'Connell, J. Cookman, J. Fallon, Ž. Krpetić and K. A. Dawson, *Nature nanotechnology*, 2015.
37. Y. Yeo, *Nanoparticulate drug delivery systems: strategies, technologies, and applications*, John Wiley & Sons, 2013.
38. M. Mammen, S.-K. Choi and G. M. Whitesides, *Angewandte Chemie International Edition*, 1998, **37**, 2754-2794.
39. D. Pozzi, V. Colapicchioni, G. Caracciolo, S. Piovesana, A. L. Capriotti, S. Palchetti, S. De Grossi, A. Riccioli, H. Amenitsch and A. Lagana, *Nanoscale*, 2014, **6**, 2782-2792.
40. R. Liu, W. Jiang, C. D. Walkey, W. C. Chan and Y. Cohen, *Nanoscale*, 2015, **7**, 9664-9675.
41. M. C. Jong, M. H. Hofker and L. M. Havekes, *Arteriosclerosis, thrombosis, and vascular biology*, 1999, **19**, 472-484.
42. S. W. Provencher, *Computer Physics Communications*, 1982, **27**, 229-242.
43. A. Calderone, L. Castagnoli and G. Cesareni, *Nature methods*, 2013, **10**, 690-691.
44. M. Ashburner, C. A. Ball, J. A. Blake, D. Botstein, H. Butler, J. M. Cherry, A. P. Davis, K. Dolinski, S. S. Dwight and J. T. Eppig, *Nature genetics*, 2000, **25**, 25-29.
45. D. Binns, E. Dimmer, R. Huntley, D. Barrell, C. O'Donovan and R. Apweiler, *Bioinformatics*, 2009, **25**, 3045-3046.
46. T. Hruz, O. Laule, G. Szabo, F. Wessendorp, S. Bleuler, L. Oertle, P. Widmayer, W. Gruissem and P. Zimmermann, *Advances in bioinformatics*, 2008, **2008**.